

# Acoustic Measurements of Critical Points for 4-Component Mixtures in Hydroformylation Reactions in Carbon Dioxide

Jie Ke <sup>a</sup>, Buxing Han <sup>b</sup>, Michael W. George <sup>a</sup>, Haike Yan <sup>b</sup>, Martyn Poliakoff <sup>a,\*</sup>

<sup>a</sup> School of Chemistry, University of Nottingham, University Park, Nottingham, NG7 2RD, UK;

(Website: <http://www.nottingham.ac.uk/supercritical>);

<sup>b</sup> Institute of Chemistry, Chinese Academy of Sciences, Beijing 100080, P. R. China

## Abstract

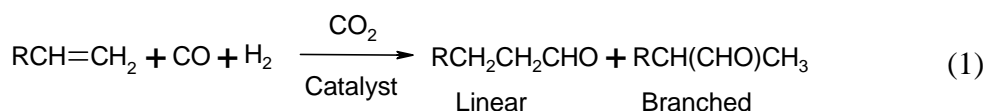
A simple acoustic technique has been used to study the vapour-liquid critical points of the reaction mixtures of hydroformylation in carbon dioxide. The systems  $\text{CO}_2 + \text{CO} + \text{H}_2 + \text{propene}$  and  $\text{CO}_2 + \text{CO} + \text{H}_2 + \text{hex-1-ene}$  have been investigated. These two quaternary systems were measured by the pseudo-binary approach (i.e. the ratio of alkene, CO and  $\text{H}_2$  being held constant). The effects of the solutes (alkene, CO and  $\text{H}_2$ ) on the critical points in the  $\text{CO}_2$ -rich fluids are discussed.

**Keywords:** Alkene; Critical state; Hydroformylation; Mixtures; Vapour-liquid equilibria; Velocity of sound

## 1. Introduction

There is increasing interest in the use of supercritical fluids (SCFs), particularly supercritical CO<sub>2</sub> (scCO<sub>2</sub>), as environmentally more acceptable solvents for reaction chemistry [1]. At the same time, it has been discovered that SCFs can provide increased control over reaction conditions and hence improved selectivity in the reaction itself [2]. A key factor in such SCF reactions is establishing whether a particular reaction mixture is homogenous or multiphase, because phase separation can alter the outcome of the reaction [3]. Despite this importance of phase behaviour, the critical points of relatively few reaction mixtures have been measured [4].

In this paper, we describe the measurement of the critical points of mixture for two different reactions in scCO<sub>2</sub>, namely the hydroformylation of propene (C<sub>3</sub>H<sub>6</sub>) and hex-1-ene (C<sub>6</sub>H<sub>12</sub>). Hydroformylation reactions are of considerable industrial importance [5]. Most of the research in SCF hydroformylation has focus on the reactions of n-alkenes, where the objective is to maximise the yield of the linear aldehyde products, Eq. (1).



Homogenous catalysis in SCFs has recently been reviewed in great detail [6]. The hydroformylation of propene in scCO<sub>2</sub> was first reported by Rathke and co-workers [7], and has since been studied by Akgerman [8]. Most recently the reaction has been carried out using homogeneous catalysts immobilised on silica [9]. Hydroformylation of higher alkenes has also been investigated by several groups [10, 11]. Here we use hex-1-ene as representative of the heavier alkenes for the measurement of phase

behaviour. The supercritical hydroformylation of hex-1-ene has already been reported by Cole-Hamilton and co-workers [12].

Although much effort has been devoted to the development of homogeneous catalysts which are soluble in  $\text{scCO}_2$ , we believe this is the first experimental study of the reaction mixtures themselves. The probable reason for this is that the reaction involves quaternary mixtures ( $\text{CO}_2 + \text{CO} + \text{H}_2 + \text{alkene}$ ) and measuring the critical points of such mixtures by traditional methods is difficult. We have used a somewhat unconventional approach, measurement of the speed of sound. Over the past 4 years, we have investigated the use of acoustic measurements for locating the critical points of mixtures [13-16]. Strictly, the velocity of sound is only a minimum at the critical point of a pure substance [17]. However, we have shown that, in practice, the minimum lies very close to the critical points of binary and ternary mixtures; sufficiently close, in fact, for the acoustic measurements to provide an experimentally acceptable estimate of the critical point. In this paper, we extend the experiment, for the first time, to quaternary mixtures.

## **2. Experimental Section**

### *2.1. Apparatus and the Method of Preparing Samples.*

The measurements were made using an acoustic technique, which can be regarded as a non-visual synthetic method [18]. The phase transition of a sample with a constant overall composition can be detected by the changes of the sound velocity. The apparatus employed in this work has been described in detail elsewhere [13, 15]. The acoustic cell is constructed from two Swagelok 1/4-inch-cross-pieces with the volume of about  $4 \text{ cm}^3$ . An acoustic signal is provided by a pulse generator, which produces a  $1 \text{ }\mu\text{s}$  width ultrasonic pulse at a repetition rate of about 100 Hz. The resulting signal is

amplified and displayed on an oscilloscope, from which the transit time of the pulse travelling between the transducers is obtained. A high pressure pump is used to adjust the system pressure to the desired value within  $\pm 0.01$  MPa. The acoustic cavity is mounted in an insulated aluminium jacket, the temperature of which is controlled within  $\pm 0.1$  K by a circulating water / glycol thermostat. The pump and acoustic cavity are held at the same temperature.

Samples of multicomponent mixtures were prepared as follows. Initially, the apparatus was purged with  $\text{CO}_2$  for 10 minutes. A measured weight of the heavy component, i.e., hex-1-ene, was added as a liquid to the cell by a syringe. Then gases, such as  $\text{C}_3\text{H}_6$ ,  $\text{CO}$  and  $\text{H}_2$  were added from high pressure reservoirs. The amount of gas was calculated from the pressure, temperature and total volume of the system. The cell and pump were kept at a constant, known temperature during this process. Finally,  $\text{CO}_2$  was expanded into the system from a high pressure bomb. The mass difference of the bomb was used to determine the amount of  $\text{CO}_2$ . The fluid was compressed and expanded inside the cell and pump for at least 6 hours to ensure adequate mixing of the sample. The temperature and pressure of the system were kept high enough to ensure no phase separation occurred. Before starting the measurement, the system was allowed to equilibrate for 30 minutes at the desired temperature. The time delay was measured as a function of pressure along each isotherm. The mixing procedure was repeated after changing the temperature to guarantee that a homogeneous liquid phase was present prior to any experiments. The error for the composition of  $\text{C}_3\text{H}_6$  /  $\text{CO}$  /  $\text{H}_2$  is essentially due to pressure measurements, which is about  $\pm 0.01$  MPa. The error on the gravimetric measurements was  $\pm 0.1$  mg for hex-1-ene and  $\pm 10$  mg for  $\text{CO}_2$ .

## 2.2. Materials

Carbon monoxide (Air Products, purity 99.8%), propene, carbon dioxide and hydrogen (BOC, purities of 99.8%, 99.99% and 99.995%, respectively) and hex-1-ene (Aldrich, purity stated higher than 97%) were used as supplied.

## 3. Results and Discussion

### 3.1. Critical Points of ternary systems

Four ternary systems ( $\text{CO}_2 + \text{C}_3\text{H}_6 + \text{CO}$ ), ( $\text{CO}_2 + \text{C}_3\text{H}_6 + \text{H}_2$ ), ( $\text{CO}_2 + \text{C}_6\text{H}_{12} + \text{CO}$ ) and ( $\text{CO}_2 + \text{C}_6\text{H}_{12} + \text{H}_2$ ) were investigated by the pseudo-binary approach. The molar ratio of alkene to CO or  $\text{H}_2$  was held at 1 : 1 for each mixture. The ternary critical data are given in Table 1.

Graphical representation of a ternary mixture is quite complicated. The four key variables i.e., temperature, pressure and the mole fractions of two of the components, cannot be represented simultaneously in 3 dimensions. Since our ternary systems have been measured by the pseudo-binary approach, only three projections,  $P$ - $x_t$ ,  $T$ - $x_t$  and  $P$ - $T$  of the critical lines are needed to represent experimental data, where  $x_t$  is the total mole fraction of solute (alkene + CO or alkene +  $\text{H}_2$ ). Fig. 1 shows the critical lines for all our ternary data. The critical points for each pseudo-binary system lie on a continuous line, which starts from the critical point of pure  $\text{CO}_2$  (see Fig. 1(b)). Within the mole fraction ranges studied here, it can be seen from Fig. 1(a) that the critical pressure for all ternary systems increases with an increase of  $x_t$ . Also, Fig. 1(c) shows that the critical temperature of two systems involving hex-1-ene increases as  $x_t$  increases. However, the critical temperature decreases with  $x_t$  for the system ( $\text{CO}_2 + \text{C}_3\text{H}_6 + \text{CO}$ ) and it is only slightly dependent on  $x_t$  for the system ( $\text{CO}_2 + \text{C}_3\text{H}_6 + \text{H}_2$ ). For a given  $x_t$ , both the critical temperature and pressure of the mixtures with hex-1-ene are higher than those of

the corresponding mixtures with propene. Moreover, for a given alkene, the critical temperatures and pressures of the ternary mixtures with  $H_2$  are higher than those with CO.

### 3.2. Critical points of the quaternary system $CO_2 + C_3H_6 + CO + H_2$

Like the ternary systems, the critical points of the quaternary system were determined by a pseudo-binary approach. For these systems, three substances ( $C_3H_6$ , CO and  $H_2$ ) were regarded as a single pseudo-component and the molar ratio  $C_3H_6 : CO : H_2$ , was held constant throughout a particular series of measurements. Our goal has been to study the effects of the solutes i.e.  $C_3H_6$ , CO and  $H_2$  on the critical points of  $CO_2$ -rich fluids, especially the effects of the concentration of permanent gases (CO and / or  $H_2$ ) in the pseudo-component ( $C_3H_6 + CO + H_2$ ). Five series of mixtures with the ratios 1 : 1 : 0.5, 1 : 1 : 1, 1 : 1 : 2, 1 : 0.5 : 1 and 1 : 1 : 2 ( $C_3H_6 : CO : H_2$ ) were studied. The mole fractions of  $CO_2$  in the mixtures varied from 0.78 to 0.96. The compositions, critical temperature and pressure for each mixture are listed in Table 2. It should be noted that the critical temperature for these quaternary mixtures is lower than that of pure  $CO_2$  (304.2 K), but the critical pressure is greater than that of  $CO_2$  (7.38 MPa).

Fig. 2 compares the critical points with the ratio of  $C_3H_6$  to CO of 1 : 1 in the pseudo-component ( $C_3H_6 + CO + H_2$ ). The ternary data of  $CO_2 + C_3H_6 + CO$  are also depicted in Fig. 2. The critical pressure not only increases with the increase of  $x_t$ , but changes with the ratio of  $H_2$ , see Fig. 2(a). In the most of cases, the more  $H_2$  in the pseudo-component, the higher is critical pressure of the mixtures. It can be seen from Fig. 2(c) that the critical temperature is a function of  $x_t$ , and it changes only slightly with the ratio of  $H_2$  in the pseudo-component.

Fig. 3 shows the experimental critical points when the ratio of  $C_3H_6$  to  $H_2$  is fixed at 1 : 1 in the pseudo-component and the mole fraction of CO is increased. For each ratio of CO in the pseudo-component, the critical pressure varies linearly with  $x_t$ , with a similar slope (Fig. 3(a)). However, it can be seen from Fig. 3(c) that the critical temperature is strongly dependent on the ratio of CO. For example, the critical temperature of mixtures with the ratio 1 : 2 : 1 ( $C_3H_6$  : CO :  $H_2$ ) is lower than that of pure  $CO_2$  (304.2 K); but the critical temperature is above 304.2 K for mixtures without CO.

### 3.3. Critical points of the quaternary system $CO_2 + C_6H_{12} + CO + H_2$

The same strategy was employed to study the quaternary system ( $CO_2 + C_6H_{12} + CO + H_2$ ). All data for this system are summarised in Table 3. In contrast to the corresponding  $C_3H_6$  system, the critical temperatures of the mixtures are higher than that of pure  $CO_2$  because the critical temperature is higher for pure hex-1-ene (504 K) than for pure  $C_3H_6$  (365 K). Data for the ratios of  $C_6H_{12}$  to CO of 1 : 1 and  $C_6H_{12}$  to  $H_2$  of 1 : 1 in the pseudo-component ( $C_6H_{12} + CO + H_2$ ) are shown in Figs. 4 and 5, respectively. The effect of CO or  $H_2$  on the critical pressure of this quaternary system (Figs. 4(a) and 5(a)) is very similar to that in the propene system. Furthermore, the critical temperature decreases with an increase in the ratio of  $H_2$  at a given  $x_t$ , as shown in Fig. 4(c). Again, the critical temperature of mixtures with high ratios of CO are shifted to lower temperature compared to the critical temperature of the ternary system ( $CO_2 + C_6H_{12} + CO$ ) (see Fig. 5(c)).

Although six binary sub-systems are involved in the quaternary system ( $CO_2 + \text{alkene} + CO + H_2$ ), the binary systems containing  $CO_2$ , i.e.  $CO_2 + \text{alkene}$ ,  $CO_2 + CO$  and  $CO_2 + H_2$  are more important than the others because the mole fraction of  $CO_2$  in

the mixtures studied here is higher than 0.8. Fig. 6 shows the comparison of the quaternary data with those for the binary sub-systems. According to the study by Haselden et al.[19], ( $\text{CO}_2 + \text{C}_3\text{H}_6$ ) shows Type I phase behaviour in the Konynenburg and Scott classifications[20]. The critical points of the binary mixtures containing  $\text{CO}_2$  and either CO or  $\text{H}_2$  shift to lower temperature and higher pressure in the  $\text{CO}_2$ -rich region[21]. We find that the CO and  $\text{H}_2$  play a dominant role in the quaternary system ( $\text{CO}_2 + \text{C}_3\text{H}_6 + \text{CO} + \text{H}_2$ ) since the critical points shift significantly towards low temperatures compared to the system ( $\text{CO}_2 + \text{C}_3\text{H}_6$ ). The binary mixture ( $\text{CO}_2 + \text{C}_6\text{H}_{12}$ ) is complete miscible at all compositions [22]. But relatively strong interaction between molecules of hex-1-ene and  $\text{CO}_2$  results in a pronounced pressure maximum on the critical line. This implies that both critical temperature and pressure are increased as the mole fraction of hex-1-ene in the  $\text{CO}_2$ -rich region. In this case, the critical temperature of the quaternary mixture with the ratio 1: 1: 1 ( $\text{C}_6\text{H}_{12} : \text{CO} : \text{H}_2$ ) is higher than that of pure  $\text{CO}_2$  and the critical pressure shifts to high pressure (see Fig. 6). CO and  $\text{H}_2$  could, therefore, be regarded as anti-solvent gases. Consequently, high operation pressures are required to form a favourable homogeneous at the same temperature.

## 4. Conclusions

New measurements of the critical points of two quaternary systems associated with the reaction mixture of the hydroformylation of propene and hex-1-ene are reported. The experimental data provide the opportunity to examine the effects of solutes (propene / hex-1-ene, CO and  $\text{H}_2$ ) on the critical points in  $\text{CO}_2$ -rich fluids. Furthermore, the data can be used to develop thermodynamic models to describe the phase behaviour of hydroformylation near the critical point of reaction mixtures. We



have also shown that the simple acoustic technique can be applied to measure the gas-liquid critical points of multicomponent mixtures.

## 5. List of Symbols

$C_3H_6$  propene

$C_6H_{12}$  hex-1-ene

$T$  temperature

$P$  pressure

$x$  mole fraction

$x_t$  total mole fraction of solute

### *Subscripts*

$c$  critical point

## Acknowledgements

We are very grateful to EPSRC, SmithKline Beecham and the Royal Society for financial support and acknowledge support from National Natural Science Foundation of China. We thank Mr. M. Guyler and Mr. K. Stanley for technical assistance.

## References

- [1] P. T. Anastas, T. C. Williamson, Eds., *Green Chemistry: Frontiers in Benign Chemical Synthesis*, Oxford University Press, Oxford, 1998.
- [2] M. G. Hitzler, F. R. Smail, S. K. Ross, M. Poliakoff, *Org. Process Res. Dev.* 2 (1998) 137-146.
- [3] W. K. Gray, M. Poliakoff, to be published.
- [4] R. J. Sadus, *AIChE J.* 40 (1994) 1376-1403.
- [5] B. Cornils, W. A. Herrmann, Eds., *Applied Homogeneous Catalysis with Organometallic Compounds, Vol. 1*, VCH, Weinheim, 1996.
- [6] P. G. Jessop, T. Ikariya, R. Noyori, *Chem. Rev.* 99 (1999) 475-494.
- [7] J. W. Rathke, R. J. Klingler, T. R. Krause, *Organometallics* 10 (1991) 1350-1355.
- [8] Y. Guo, A. Akgerman, *Ind. Eng. Chem. Res.* 36 (1997) 4581-4585.
- [9] N. J. Meehan, A. J. Sandee, J. N. H. Reek, P. J. C. Kamer, P. W. M. N. van Leeuwen, M. Poliakoff, *Chem. Commun. submitted* (2000) .
- [10] D. Koch, W. Leitner, *J. Am. Chem. Soc.* 120 (1998) 13398-13404.
- [11] D. R. Palo, C. Erkey, *Organometallics* 19 (2000) 81-86.
- [12] I. Bach, D. J. Cole-Hamilton, *Chem. Commun.* (1998) 1463-1464.
- [13] A. Kordikowski, D. G. Robertson, A. I. Aguiar-Ricardo, V. K. Popov, S. M. Howdle, M. Poliakoff, *J. Phys. Chem.* 100 (1996) 9522-9526.
- [14] A. Kordikowski, D. G. Robertson, M. Poliakoff, *Anal. Chem.* 68 (1996) 4436-4440.

- [15] A. Kordikowski, D. G. Robertson, M. Poliakoff, T. D. DiNoia, M. McHugh, A. Aguiar-Ricardo, *J. Phy. Chem. B* 101 (1997) 5853-5862.
- [16] A. Kordikowski, M. Poliakoff, *Fluid Phase Equilib.* 151 (1998) 493-499.
- [17] J. S. Rowlinson, F. L. Swinton, *Liquids and Liquid Mixtures*, Butterworth, London, 1982.
- [18] D. Dohrn, G. Brunner, *Fluid Phase Equilib.* 106 (1995) 213-282.
- [19] G. G. Haselden, D. M. Newitt, S. M. Shah, *Proc. Roy. Soc. A.* 209 (1951) 1-14.
- [20] P. H. Van Konynenburg, R. L. Scott, *Philos. Trans. R. Soc. London, Ser. A* 298 (1980) 495-540.
- [21] B. Han, M. Poliakoff, unpublished results.
- [22] F. Leder, C. A. Irani, *J. Chem. Eng. Data* 20 (1975) 323-327.
- [23] The critical line was calculated from the Peng-Robinson equation of state [24] with a computational algorithm developed by Heidemann and Khalil [25]. The interaction parameters were obtained by fitting experimental data from the literature.
- [24] D.-Y. Peng, D. B. Robinson, *Ind. Eng. Chem. Fundam.* 15 (1976) 59-64.
- [25] R. A. Heidemann, A. M. Khalil, *AIChE J.* 26 (1980) 769-779.

Table 1 Critical points <sup>a</sup> for the ternary systems CO<sub>2</sub>(1)<sup>b</sup> + C<sub>3</sub>H<sub>6</sub>(2) + CO(3) <sup>c</sup>, CO<sub>2</sub>(1) + C<sub>3</sub>H<sub>6</sub>(2) + H<sub>2</sub>(3), CO<sub>2</sub>(1) + C<sub>6</sub>H<sub>12</sub>(2) + CO(3) and CO<sub>2</sub>(1) + C<sub>6</sub>H<sub>12</sub>(2) + H<sub>2</sub>(3)

$x_2$	$x_3$	$T_c / \text{K}$	$P_c / \text{MPa}$
CO <sub>2</sub> (1) + C <sub>3</sub> H <sub>6</sub> (2) + CO(3)			
0.023	0.023	303.3	7.52
0.050	0.050	301.7	7.73
0.066	0.066	300.7	7.83
0.086	0.086	299.2	7.98
CO <sub>2</sub> (1) + C <sub>3</sub> H <sub>6</sub> (2) + H <sub>2</sub> (3)			
0.029	0.029	305.0	8.36
0.052	0.052	305.4	9.06
CO <sub>2</sub> (1) + C <sub>6</sub> H <sub>12</sub> (2) + CO(3)			
0.022	0.022	308.6	8.04
0.029	0.029	309.5	8.26
0.048	0.048	311.9	8.70
0.066	0.066	313.8	9.35
0.090	0.090	316.9	10.20
CO <sub>2</sub> (1) + C <sub>6</sub> H <sub>12</sub> (2) + H <sub>2</sub> (3)			
0.026	0.026	312.4	8.89
0.039	0.039	316.1	9.61
0.068	0.068	320.6	10.98

<sup>a</sup> Error for  $T_c$  and  $P_c$  are  $\pm 0.3$  K and  $\pm 0.04$  MPa, respectively. <sup>b</sup> The figure in parentheses is the component number of compound which precedes it. <sup>c</sup>  $x_2 : x_3 = 1 : 1$ .

Table 2 Critical points <sup>a</sup> for the quaternary system CO<sub>2</sub> + C<sub>3</sub>H<sub>6</sub> + CO + H<sub>2</sub>

$x_{\text{C}_3\text{H}_6}$	$x_{\text{CO}}$	$x_{\text{H}_2}$	$T_c / \text{K}$	$P_c / \text{MPa}$
$x_{\text{C}_3\text{H}_6} : x_{\text{CO}} : x_{\text{H}_2} = 1 : 1 : 0.5$				
0.024	0.024	0.012	302.4	7.92
0.034	0.034	0.017	301.6	8.24
0.057	0.057	0.029	299.6	8.73
0.071	0.071	0.036	298.6	9.12
$x_{\text{C}_3\text{H}_6} : x_{\text{CO}} : x_{\text{H}_2} = 1 : 1 : 1$				
0.014	0.014	0.014	303.2	8.02
0.018	0.018	0.018	302.9	8.11
0.029	0.029	0.029	301.9	8.55
0.049	0.049	0.049	299.9	9.21
0.065	0.065	0.065	298.0	9.83
$x_{\text{C}_3\text{H}_6} : x_{\text{CO}} : x_{\text{H}_2} = 1 : 1 : 2$				
0.013	0.013	0.026	303.2	7.92
0.024	0.024	0.049	301.7	8.48
0.037	0.037	0.073	299.5	9.32
0.055	0.055	0.109	296.8	10.85
$x_{\text{C}_3\text{H}_6} : x_{\text{CO}} : x_{\text{H}_2} = 1 : 0.5 : 1$				
0.018	0.009	0.018	304.0	8.06
0.038	0.019	0.038	303.0	8.77
0.053	0.026	0.053	302.3	9.24
0.075	0.037	0.075	301.4	9.85
$x_{\text{C}_3\text{H}_6} : x_{\text{CO}} : x_{\text{H}_2} = 1 : 2 : 1$				
0.011	0.022	0.011	302.5	7.91
0.018	0.036	0.018	301.4	8.26
0.027	0.053	0.027	299.3	8.68
0.035	0.069	0.035	297.6	9.00
0.050	0.100	0.050	295.3	9.70

<sup>a</sup> Error for  $T_c$  and  $P_c$  are  $\pm 0.3$  K and  $\pm 0.04$  MPa, respectively.

Table 3 Critical points <sup>a</sup> for the quaternary system CO<sub>2</sub> + C<sub>6</sub>H<sub>12</sub> + CO + H<sub>2</sub>

$x_{\text{C}_6\text{H}_{12}}$	$x_{\text{CO}}$	$x_{\text{H}_2}$	$T_c / \text{K}$	$P_c / \text{MPa}$
$x_{\text{C}_6\text{H}_{12}} : x_{\text{CO}} : x_{\text{H}_2} = 1 : 1 : 0.5$				
0.020	0.020	0.010	307.8	8.39
0.038	0.038	0.019	310.3	9.20
0.051	0.051	0.026	311.5	9.87
0.067	0.067	0.034	312.1	10.70
0.076	0.076	0.038	312.5	10.99
$x_{\text{C}_6\text{H}_{12}} : x_{\text{CO}} : x_{\text{H}_2} = 1 : 1 : 1$				
0.018	0.018	0.018	308.2	8.78
0.036	0.036	0.036	310.3	10.11
0.054	0.054	0.054	311.2	11.40
$x_{\text{C}_6\text{H}_{12}} : x_{\text{CO}} : x_{\text{H}_2} = 1 : 1 : 2$				
0.012	0.012	0.024	306.8	8.77
0.021	0.021	0.041	308.2	9.62
0.034	0.034	0.068	309.7	11.03
0.041	0.041	0.081	310.3	12.04
$x_{\text{C}_6\text{H}_{12}} : x_{\text{CO}} : x_{\text{H}_2} = 1 : 0.5 : 1$				
0.021	0.010	0.021	310.1	8.71
0.042	0.021	0.042	312.9	9.68
0.061	0.030	0.061	315.1	10.75
$x_{\text{C}_6\text{H}_{12}} : x_{\text{CO}} : x_{\text{H}_2} = 1 : 2 : 1$				
0.013	0.026	0.013	306.5	8.52
0.025	0.049	0.025	305.8	9.38
0.038	0.075	0.038	305.0	10.60

<sup>a</sup> Error for  $T_c$  and  $P_c$  are  $\pm 0.3$  K and  $\pm 0.04$  MPa, respectively.

## Figure Caption

Fig. 1. The critical points of the ternary systems at the fixed ratio  $x_2 : x_3 = 1:1$  : (a)  $P$ - $x_t$  projection, (b)  $P$ - $T$  projection (c)  $T$ - $x_t$  projection. ( $\square$ ) ( $\text{CO}_2 + \text{C}_3\text{H}_6 + \text{CO}$ ), ( $\circ$ ) ( $\text{CO}_2 + \text{C}_3\text{H}_6 + \text{H}_2$ ), ( $\blacksquare$ ) ( $\text{CO}_2 + \text{C}_6\text{H}_{12} + \text{CO}$ ), ( $\bullet$ ) ( $\text{CO}_2 + \text{C}_6\text{H}_{12} + \text{H}_2$ ), (—) curves fitted to experimental data.

Fig. 2. The critical points of the quaternary system ( $\text{CO}_2 + \text{C}_3\text{H}_6 + \text{CO} + \text{H}_2$ ) at the fixed ratio of  $\text{C}_3\text{H}_6$  to  $\text{CO}$ : (a)  $P$ - $x_t$  projection, (b)  $P$ - $T$  projection (c)  $T$ - $x_t$  projection. The molar ratios  $\text{C}_3\text{H}_6 : \text{CO} : \text{H}_2$  are ( $\square$ )  $1 : 1 : 0$ , ( $\circ$ )  $1 : 1 : 0.5$ , ( $\Delta$ )  $1 : 1 : 1$ , ( $\diamond$ )  $1 : 1 : 2$ . (—) curves fitted to experimental data.

Fig. 3. The critical points of the quaternary system ( $\text{CO}_2 + \text{C}_3\text{H}_6 + \text{CO} + \text{H}_2$ ) at the fixed ratio of  $\text{C}_3\text{H}_6$  to  $\text{H}_2$ : (a)  $P$ - $x_t$  projection, (b)  $P$ - $T$  projection (c)  $T$ - $x_t$  projection. The molar ratios  $\text{C}_3\text{H}_6 : \text{CO} : \text{H}_2$  are ( $\square$ )  $1 : 0 : 1$ , ( $\circ$ )  $1 : 0.5 : 1$ , ( $\Delta$ )  $1 : 1 : 1$ , ( $\diamond$ )  $1 : 2 : 1$ . (—) curves fitted to experimental data.

Fig. 4. The critical points of the quaternary system ( $\text{CO}_2 + \text{C}_6\text{H}_{12} + \text{CO} + \text{H}_2$ ) at the fixed ratio of  $\text{C}_6\text{H}_{12}$  to  $\text{CO}$ : (a)  $P$ - $x_t$  projection, (b)  $P$ - $T$  projection (c)  $T$ - $x_t$  projection. The molar ratios  $\text{C}_6\text{H}_{12} : \text{CO} : \text{H}_2$  are ( $\square$ )  $1 : 1 : 0$ , ( $\circ$ )  $1 : 1 : 0.5$ , ( $\Delta$ )  $1 : 1 : 1$ , ( $\diamond$ )  $1 : 1 : 2$ . (—) curves fitted to experimental data.

Fig. 5. The critical points of the quaternary system ( $\text{CO}_2 + \text{C}_6\text{H}_{12} + \text{CO} + \text{H}_2$ ) at the fixed ratio of  $\text{C}_6\text{H}_{12}$  to  $\text{H}_2$ : (a)  $P$ - $x_t$  projection, (b)  $P$ - $T$  projection (c)  $T$ - $x_t$  projection. The molar ratios  $\text{C}_6\text{H}_{12} : \text{CO} : \text{H}_2$  are ( $\square$ )  $1 : 0 : 1$ , ( $\circ$ )  $1 : 0.5 : 1$ , ( $\Delta$ )  $1 : 1 : 1$ , ( $\diamond$ )  $1 : 2 : 1$ . (—) curves fitted to experimental data.

Fig. 6. Comparison of two quaternary systems with binary sub-systems. ( $\Delta$ ) ( $\text{CO}_2 + \text{CO}$ ) [21], ( $\times$ ) ( $\text{CO}_2 + \text{H}_2$ ) [21], ( $\cdot - \cdot - \cdot$ ) ( $\text{CO}_2 + \text{C}_3\text{H}_6$ ) [19, 23-25], ( $\diamond$ ) ( $\text{CO}_2 + \text{C}_6\text{H}_{12}$ ) [22], ( $\circ$ ) ( $\text{CO}_2 + \text{C}_3\text{H}_6 + \text{CO} + \text{H}_2$ ), ( $\square$ ) ( $\text{CO}_2 + \text{C}_6\text{H}_{12} + \text{CO} + \text{H}_2$ ), (—) curves fitted to experimental data. The ratio alkene :  $\text{CO} : \text{H}_2 = 1 : 1 : 1$  in quaternary systems.

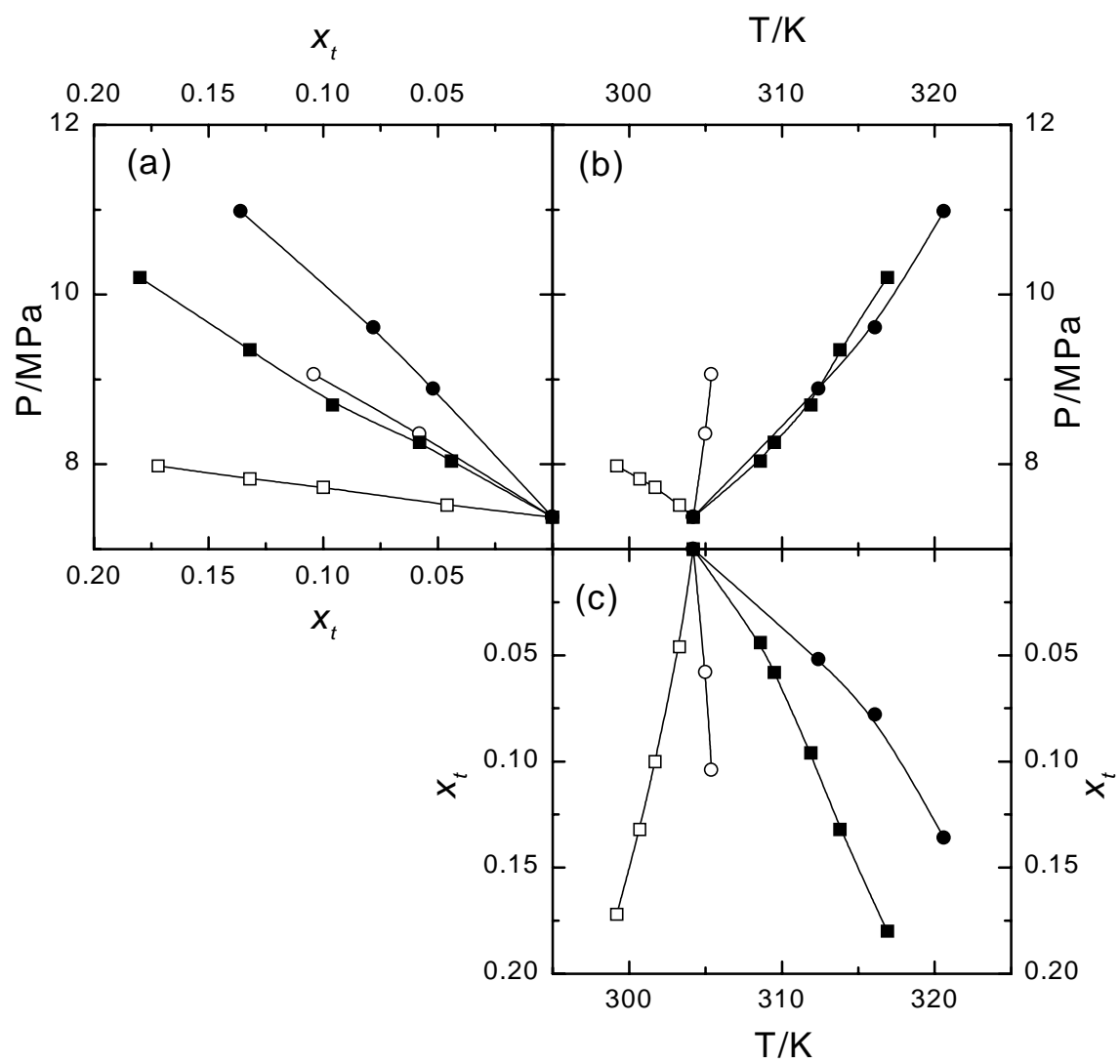


Fig. 1



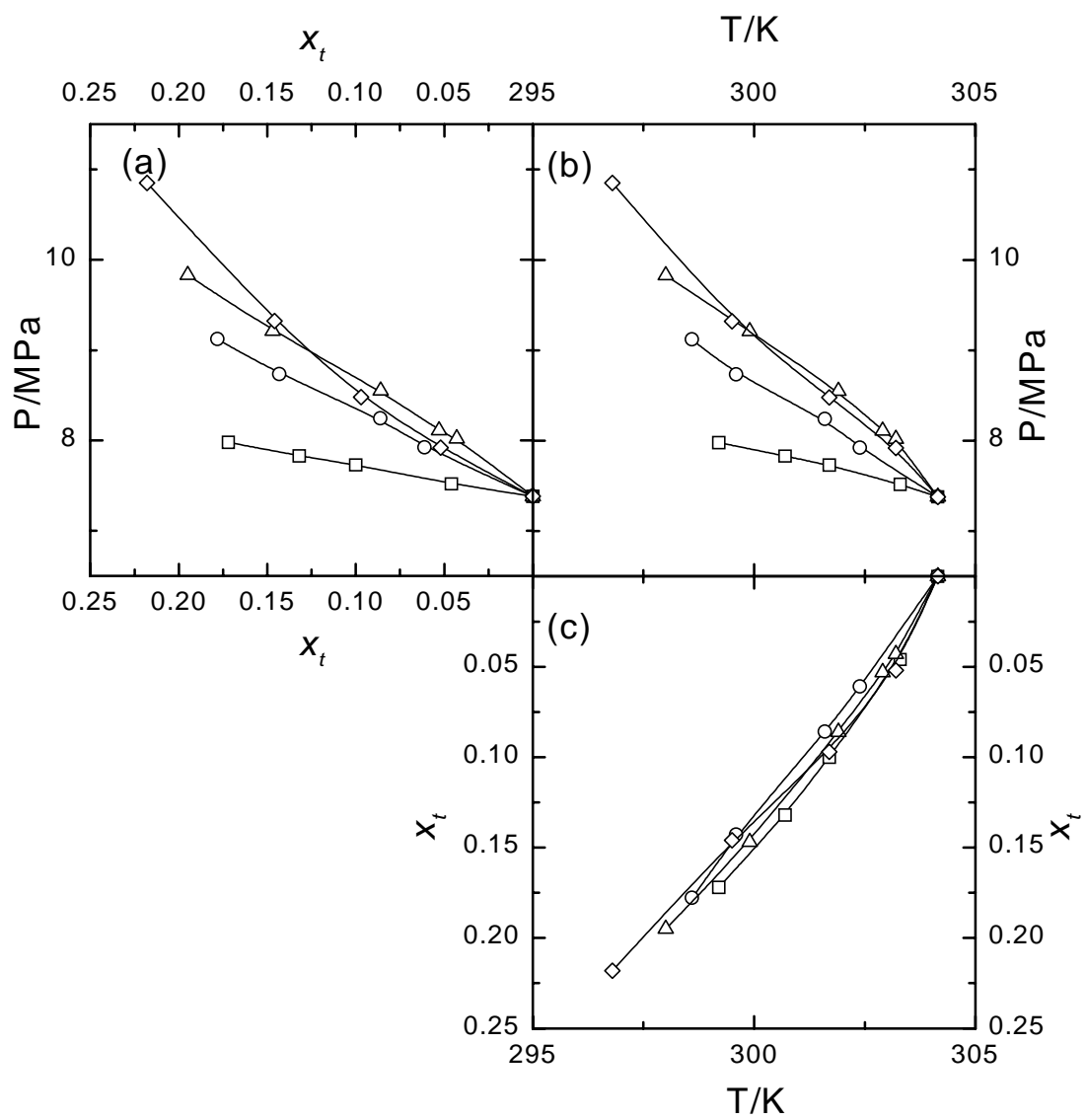


Fig. 2

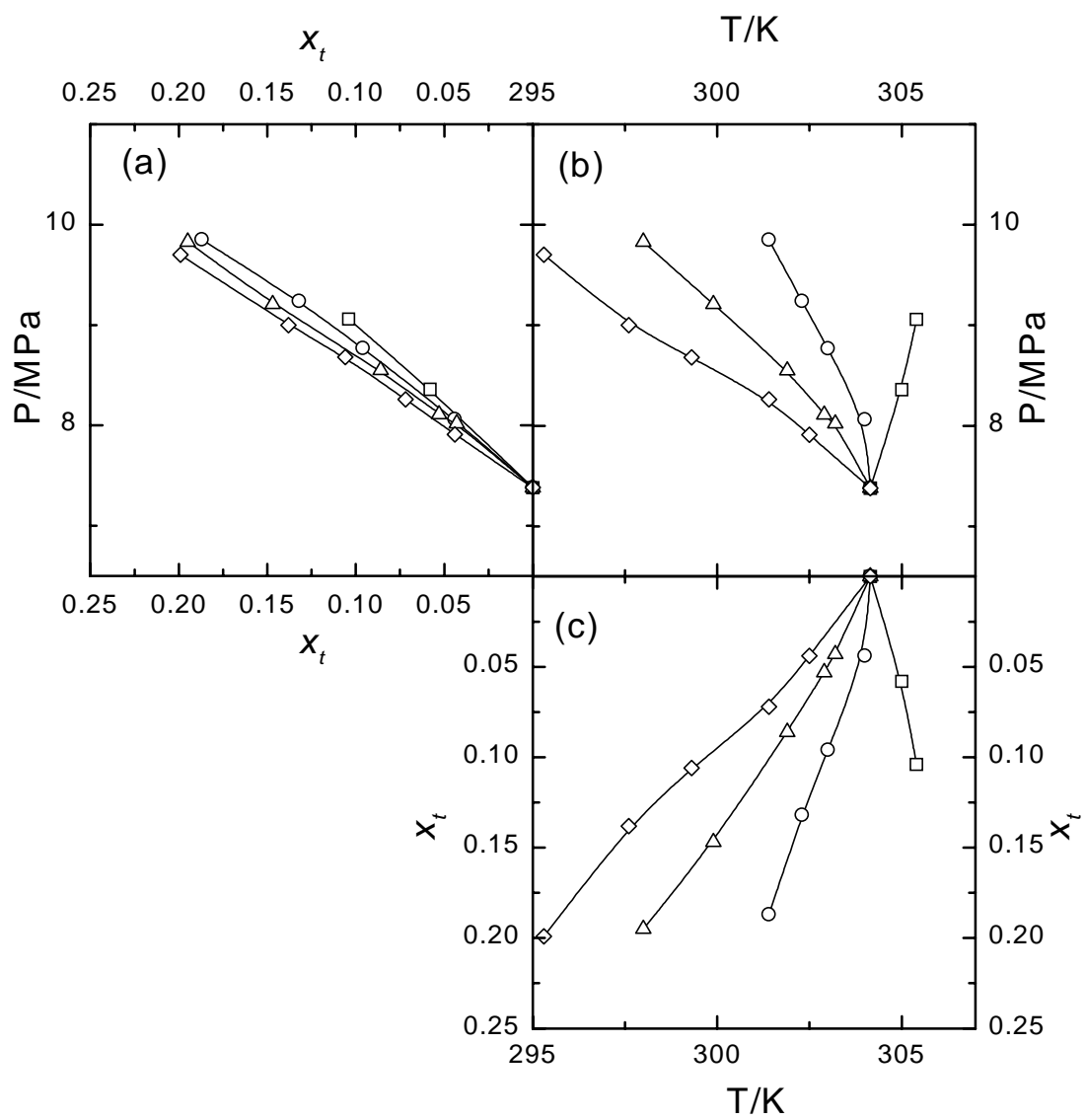


Fig. 3

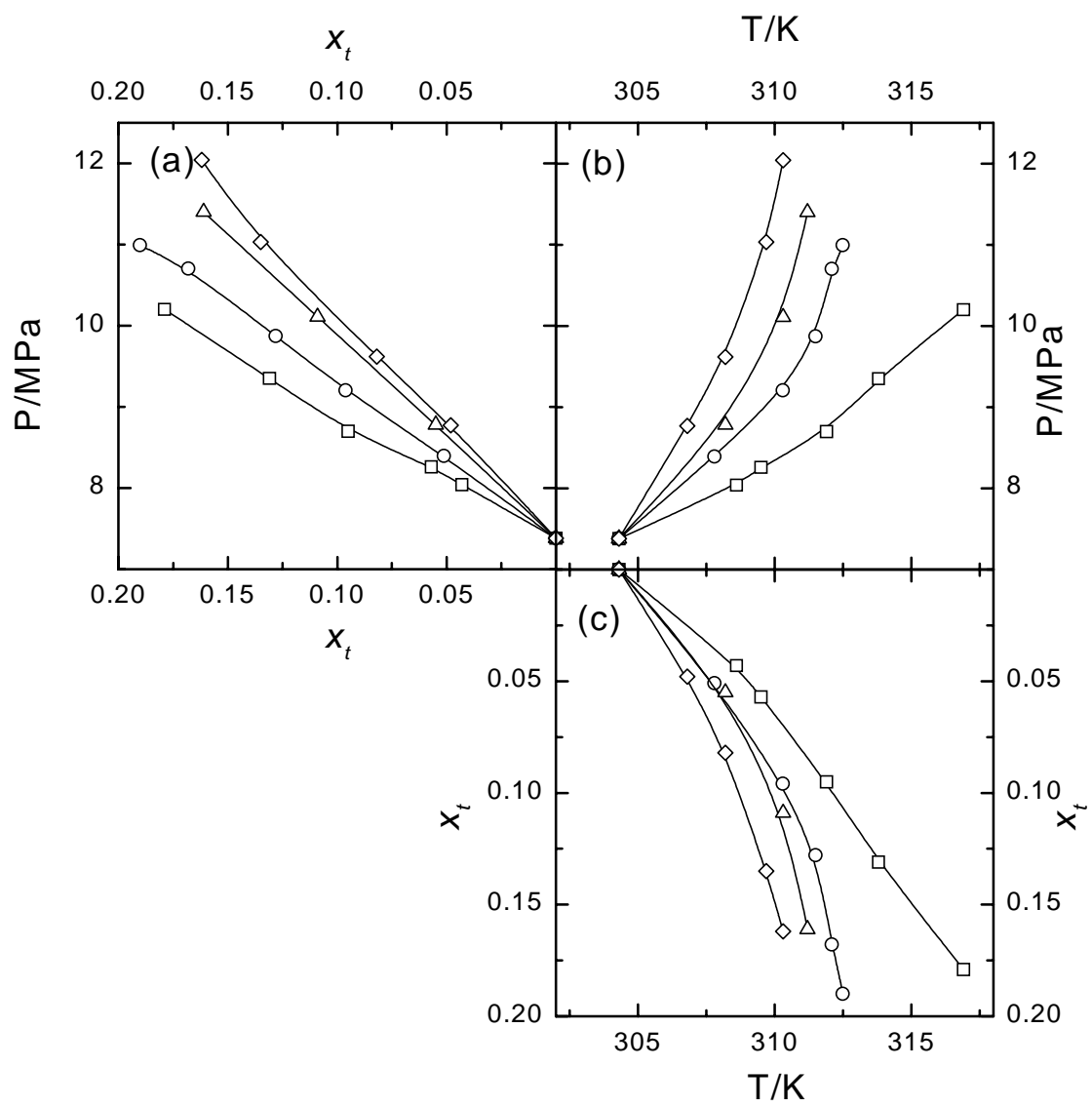


Fig. 4

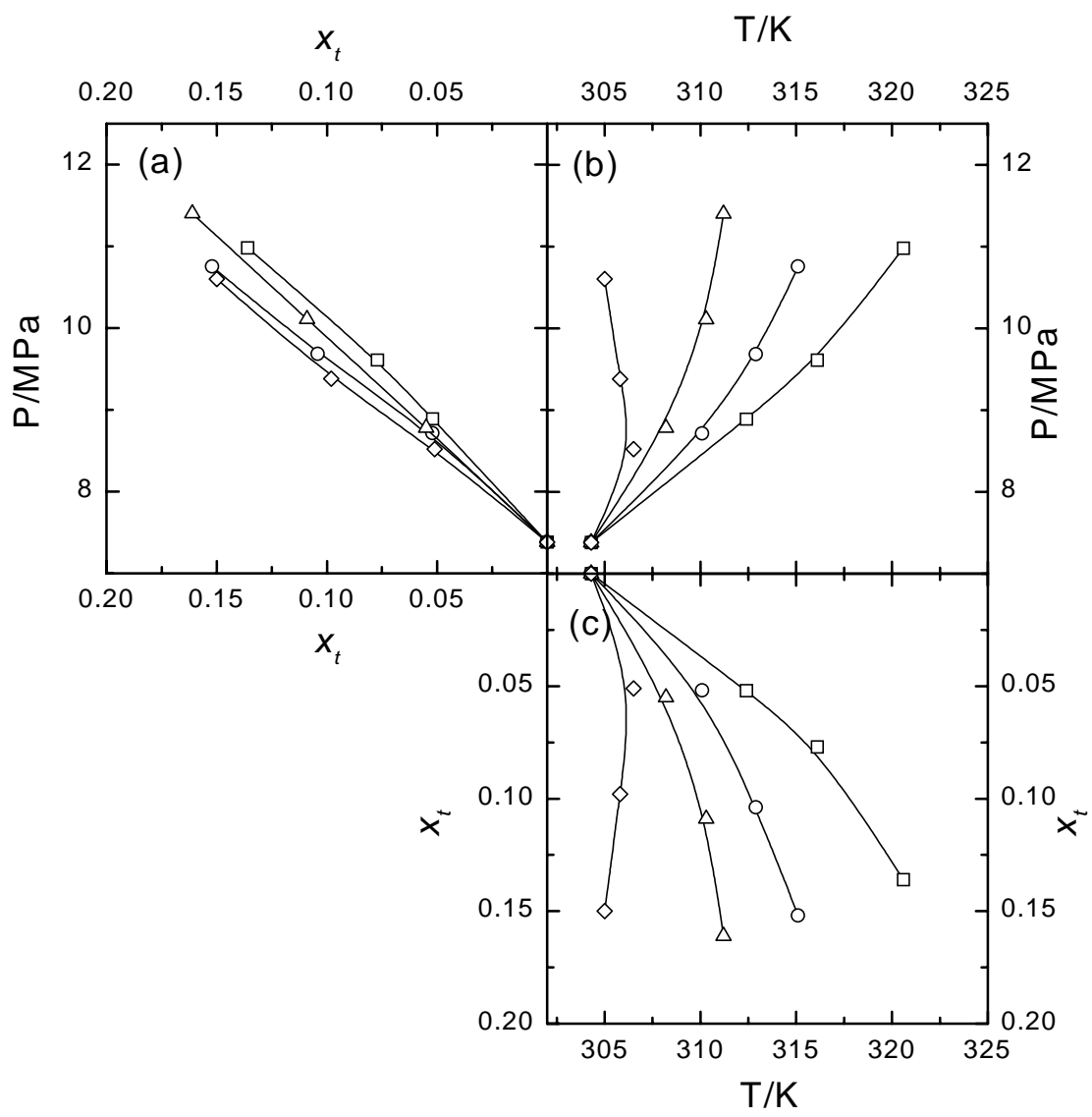


Fig. 5

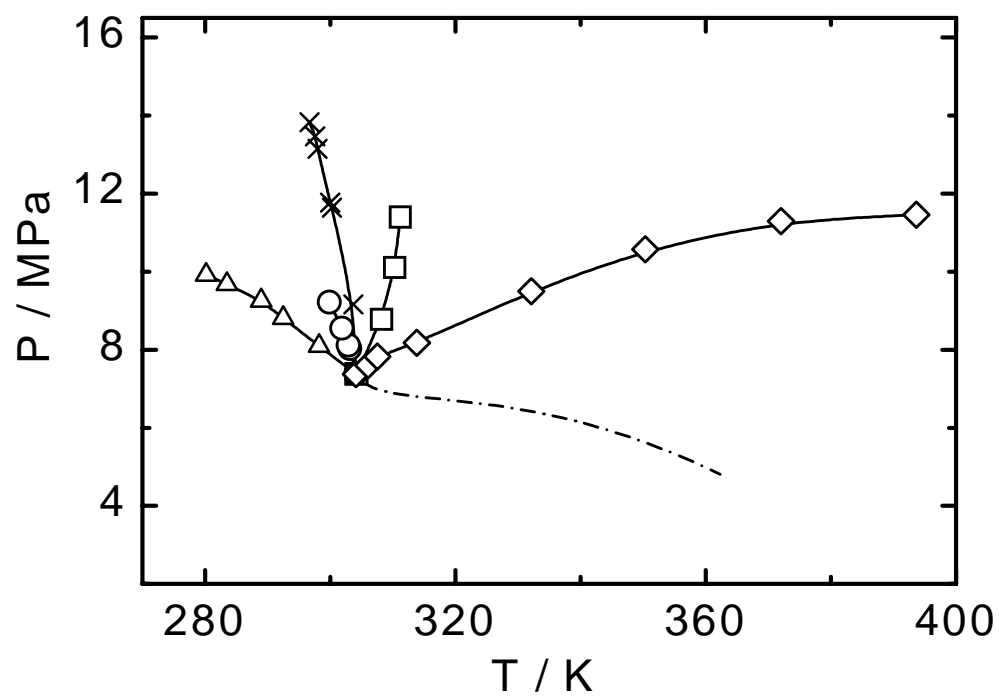


Fig. 6